



**HAL**  
open science

# Sigma Lenses: Focus-Context Transitions Combining Space, Time and Translucence

Emmanuel Pietriga, Caroline Appert

► **To cite this version:**

Emmanuel Pietriga, Caroline Appert. Sigma Lenses: Focus-Context Transitions Combining Space, Time and Translucence. CHI '08: Proceedings of the SIGCHI Conference on Human Factors in Computing Systems, ACM, Apr 2008, Florence, Italy. 10.1145/1357054.1357264 . inria-00271301

**HAL Id: inria-00271301**

**<https://inria.hal.science/inria-00271301>**

Submitted on 8 Apr 2008

**HAL** is a multi-disciplinary open access archive for the deposit and dissemination of scientific research documents, whether they are published or not. The documents may come from teaching and research institutions in France or abroad, or from public or private research centers.

L'archive ouverte pluridisciplinaire **HAL**, est destinée au dépôt et à la diffusion de documents scientifiques de niveau recherche, publiés ou non, émanant des établissements d'enseignement et de recherche français ou étrangers, des laboratoires publics ou privés.

# Sigma Lenses: Focus-Context Transitions Combining Space, Time and Translucence

Emmanuel Pietriga<sup>1,2</sup>  
emmanuel.pietriga@inria.fr

<sup>1</sup>INRIA  
Bât 490 - Orsay, F-91405, France

Caroline Appert<sup>2,1</sup>  
appert@lri.fr

<sup>2</sup>LRI - Univ. Paris-Sud & CNRS  
Bât 490 - Orsay, F-91405, France

## ABSTRACT

Focus + context techniques such as fisheye lenses are used to navigate and manipulate objects in multi-scale worlds. They provide in-place magnification of a region without requiring users to zoom the whole representation and consequently lose context. Their adoption is however hindered by usability problems mostly due to the nature of the transition between focus and context. Existing transitions are often based on a physical metaphor (magnifying glass, fisheye, rubber sheet), and are almost always achieved through a single dimension: space. We investigate how other dimensions, namely time and translucence, can be used to achieve more efficient transitions. We present an extension to Carpendale's framework for unifying presentation space accommodating these new dimensions. We define new lenses in that space, called *Sigma lenses*, and compare them to existing lenses through experiments based on a generic task: focus targeting. Results show that one new lens, the SPEED-COUPLED BLENDING lens, significantly outperforms all others.

## Author Keywords

Multi-scale interfaces, Focus + Context, Fisheye lenses, Translucence, Focus targeting, Controlled experiment

## ACM Classification Keywords

H. Information Systems H.5 Information Interfaces and Presentation H.5.2 User Interfaces (H.1.2, I.3.6)

## INTRODUCTION

Many techniques can be used in combination with classical pan & zoom to navigate large multi-scale worlds. Among them, a range of bifocal display techniques have been designed, which can be broadly categorized as either overview + detail or focus + context techniques. Overview + detail techniques [25] usually put the context view in a small inset located in a corner of the screen, leaving most of the latter to the detailed view, while focus + context techniques do the opposite: the context occupies the whole screen except for a

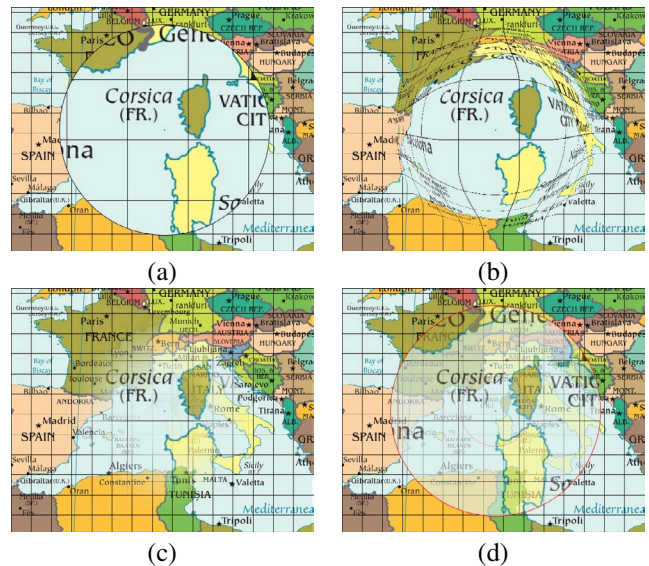


Figure 1. Various transitions between focus and context: (a) step transition causing occlusion, (b) distorting space, (c) using gradually increasing translucence, (d) using a combination of translucence and time.

small area that provides in-place magnification of a limited region of the context. While overview + detail techniques are generally favored and have been shown to perform well in some situations [16, 22, 24], there are cases where they show their limits: for instance, when navigating a map of a densely populated region to look for particular localities, overview + detail techniques can only use a few pixels to display each of them in the context view. On the contrary, focus + context techniques can convey additional information in the context view, such as the localities' names, thus providing users with more contextual information that can guide navigation. They have also been shown to perform efficiently in other situations, e.g., for large steering tasks [14] or when selecting small targets with a stylus [27].

Even though they have been studied for some time, the adoption of focus + context techniques remains limited, mostly due to comprehension and low-level interaction problems [4, 11] related to how the transition between the context and the magnified focus region is achieved. Many of the transitions described in the literature are inspired by the physical world and are presented through metaphors such as magnifying glasses, rubber sheets [30], and more generally surface deformations [3]; in other words, spatial transitions caus-

ing various problems that can hinder performance. For instance simple magnifying glasses (Figure 1-a) create occlusion of the immediate context adjacent to the magnified region [28]; graphical fisheyes [29], also known as distortion lenses (Figure 1-b), make it difficult to acquire targets [11], especially for high magnification factors. To cancel the negative effects of distortion associated with fisheyes, Gutwin proposed Speed-coupled flattening lenses [11], introducing time as a dimension to transition between focus and context. The comparison of these time-based lenses with plain fish-eye lenses demonstrated that the performance of lens-based techniques can be improved by using dimensions other than space to control the transition between focus and context.

In addition to space and time, we argue that other dimensions readily available in the electronic world can be used to provide more efficient transitions between focus and context. In this paper we introduce a generalization of Carpendale’s framework for unifying presentation space [5]. This generalization encompasses transitions based on two orthogonal dimensions: space and translucence (Figure 1-c), which can be combined with a third dimension: time (Figure 1-d). This opens up a large design space, called the *Sigma lens design space*, in which we identify interesting points. We report on the results of an evaluation of five lenses on the generic task of focus targeting, a basic motor task involved in many high-level navigation tasks. The main finding of these evaluations is that one new lens, the SPEED-COUPLED BLENDING lens, significantly outperforms all other types of lenses for that task.

## RELATED WORK

Focus + context techniques are mainly differentiated by the way they transition between the focus and context regions. Techniques such as the DragMag [32] and Manhattan lenses [5] display the focus as an inset which is offset from the corresponding context region so as not to occlude the local context adjacent to that region. In this particular case, there is no actual transition between focus and context, which are simply connected through lines serving as visual cues. Techniques that do not offset the focus region provide an *in situ* magnification that sits on top of the corresponding context region [19]. They have to use some type of transition in order to avoid occlusion of the adjacent context. This is almost always achieved by distorting the representation, so as to smoothly integrate the focus into the context. The distortion can affect the entire representation: Graphical Fisheyes [29], the Rubber Sheet [30], the Document Lens [28], the Perspective Wall [21]. Or it can be restricted to a specific region, in which case they are called constrained lenses [5, 19]. These have the advantage of distorting only a limited region around the focus, leaving most of the context untouched. They have been shown to work better than full screen lenses for some tasks [13], and should be favored when the focus has to be relocated often, as they reduce the amount of visual changes during lens movements (focus retargeting). Various improvements to these techniques have been proposed, such as ways to achieve higher magnification [6], and visual cues that can help in comprehending distortion [4]. In almost all cases, however, the transition between focus and context is achieved through one single dimension: space.

Magic Lens filters, part of the See-Through Interface [2], are powerful generic lenses that are used to modify the rendering of objects seen through them. However, to our knowledge, they have not been used to specifically address the problem of smoothly transitioning between focus and context, whether through space, time, or translucence. Lieberman used translucence in Powers of Ten Thousands [20], a bifocal display technique that makes the focus and context views share the same physical screen space, by using multiple translucent layers. But as with the DragMag, there is no actual transition between focus and context, which are overlaid on top of one another. Even though it has been shown to be usable in exploratory studies [7, 15], this type of representation based on transparent or translucent layers is cognitively demanding, causing visual interferences that are the source of serious legibility problems, and requiring additional mental effort from the user to relate focus and context. Translucence remains, however, an interesting dimension which has been used successfully to reclaim some screen real-estate, either in combination with other filters such as in multiblending [1] or by making the translucence level dynamically vary as a function of cursor movements [12]. As mentioned earlier, cursor movements have been used in a different context, closer to our problem, for controlling the magnification factor of speed-coupled flattening lenses [11] over time, with the effect of increasing focus targeting performance compared to the equivalent static fish-eye lenses. Another technique, Speed-dependent automatic zooming [17], couples zoom level in a window with scroll rate, zooming-out as speed increases. We believe that new types of lenses can be created by more systematically combining the above dimensions, namely space, translucence and time, in order to provide more efficient transitions between focus and context in multi-scale interfaces.

## SPACE, TIME, TRANSLUCENCE, AND BEYOND

The basic concepts for describing spatial distortion between focus and context have been defined in Carpendale’s framework for unifying presentation space [5]. In this section we reformulate these concepts in a slightly different, but equivalent way in order to accommodate our generalization of transitions between focus and context. This formulation is based on space-scale diagrams [9] and uses the associated terminology. Basic knowledge about these diagrams is assumed.

### General Properties

We consider the focus and context regions of any lens-based representation as separate viewing windows in a space-scale diagram. The final rendered viewing window is a composition of points from both windows.

All constrained lenses, no matter how they transition between focus and context, have the following properties:

- $MM$  : the maximum magnification in the focus region (a.k.a the flat-top),
- $R_I$  : the radius of the flat-top region, which we call *inner radius*,
- $R_O$  : the radius of the lens at its base (i.e., its extent), which we call *outer radius*,
- $(x_c, y_c)$  : the coordinates of the lens’ center.

Figure 2 illustrates these definitions using a distortion lens applied to a scene made of a series of equal-size rectangles that form a regular color spectrum. The *context viewing window* corresponds to what is seen in the absence of any lens. If it is positioned at  $s$  on scale axis  $v$ , the *focus viewing window* is necessarily positioned at  $s \cdot MM$ . Points A and B represent the boundaries of the constrained lens within the context viewing window, at a distance  $R_O$  from the lens' center C. The focus viewing window is then a flat magnification by a factor of  $MM$  of the region delimited by A and B. Its size is thus  $2 \cdot MM \cdot R_O$ .  $R_I$  controls the size of the lens' flat-top. If  $R_I = R_O$ , the lens is a mere magnifier lens (or magnifying glass) as illustrated in Figure 1-a. If  $R_I$  is zero, the flat-top is reduced to a single point at the center of the lens, which is then the only point at full magnification.

The final viewing window obtained at rendering time can be seen as a combination of the two abstract windows introduced above: the rendering of the focus window is integrated, after some transformation, in the context window.

### Spatial Transitions

The most common transformation consists in displacing all points in the focus window to achieve a smooth transition between focus and context through spatial distortion [5]. This type of transformation can be defined through a drop-off function, such as a Gaussian (see Figure 2), which models the magnification profile of the lens. Associated with a distance function  $d$ , the drop-off function is defined as:

$$\mathcal{G}_{scale} : (x, y, d) \mapsto s$$

with  $s$  a scaling factor.  $\mathcal{G}_{scale}$  is usually a monotonically decreasing function with a range of  $[1, MM]$ . This is not a strong requirement; other functions may however introduce discontinuities in the spatial transition.

The rendering of point  $(x, y)$  in the final viewing window is then defined through the displacement function  $r$ :

$$r(x, y) = \begin{cases} \left( x_c + \frac{x-x_c}{MM}, y_c + \frac{y-y_c}{MM} \right) & \{\forall(x, y) | d(x, y) \leq R_I\} \quad (1) \\ \left( x_c + \frac{x-x_c}{\mathcal{G}_{scale}(x, y, d)}, y_c + \frac{y-y_c}{\mathcal{G}_{scale}(x, y, d)} \right) & \{\forall(x, y) | R_I < d(x, y) < R_O\} \quad (2) \\ (x, y) & \{\forall(x, y) | d(x, y) \geq R_O\} \quad (3) \end{cases}$$

The flat-top region corresponds to case (1), the transition to case (2), and the region beyond the lens boundaries (i.e., the context) corresponds to case (3). Distance function  $d$  is based on  $L_p$ -metrics, and is defined as follows:

$$d : (x, y) \mapsto \sqrt[P]{|x - x_c|^P + |y - y_c|^P}$$

where  $(x, y)$  are the coordinates of a point seen through a lens centered in  $(x_c, y_c)$ , and  $P \in \mathbb{N}^*$ . Most lenses are either radial ( $P = 2$ , circular shape) or orthogonal ( $P = \infty$ , square shape). A Gaussian function is often used to define drop-off function  $\mathcal{G}_{scale}$ , as it provides one of the smoothest visual transitions between focus and context. Figures 2 and 1-b illustrate Gaussian distortion lenses. It is not the purpose of

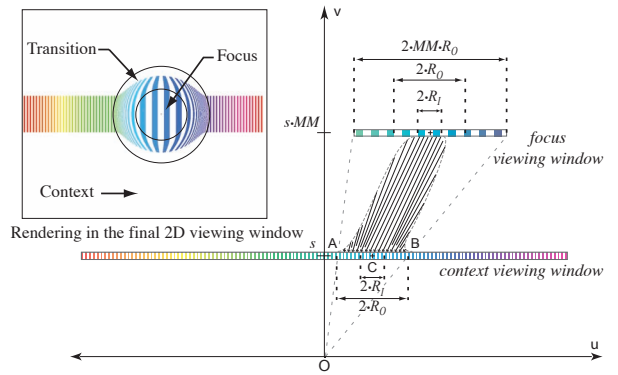


Figure 2. Gaussian distortion lens in a 1+1D space-scale diagram, and corresponding 2D rendering.

this article to provide a detailed survey of all possible drop-off and distance functions, which are already well-described in the literature [5, 6].

### Translucence as a Transition Dimension

Digital image compositing and more particularly alpha blending represents another, yet unexplored, method for transitioning between the focus and context regions of a constrained lens. As with spatial distortion, the final viewing window obtained at rendering time is a combination of the two abstract viewing windows: here, points of the focus window are composited with points of the context window. For instance, using gradually increasing translucence, it is possible to smoothly blend the focus viewing window into the context, thus achieving a transition without resorting to distortion (see Figures 3 and 1-c).

The continuity between focus and context is realized through compositing only. Given two points with  $(r, g, b)$  color components, one in the focus window and one in the context window, we note:

$$p_{context} \otimes_{\alpha} p_{focus}$$

the point  $p_{comp}$  resulting from compositing them using Porter & Duff's Source atop Destination alpha blending rule [26] with a value of  $\alpha$ , the source being the focus viewing window and the destination the context viewing window:

$$p_{comp} = \begin{pmatrix} \alpha \cdot r_{focus} + (1 - \alpha) \cdot r_{context} \\ \alpha \cdot g_{focus} + (1 - \alpha) \cdot g_{context} \\ \alpha \cdot b_{focus} + (1 - \alpha) \cdot b_{context} \end{pmatrix}$$

As with scale for distortion lenses, the translucence profile can be defined by a drop-off function that maps a translucence level to a point  $(x, y)$  located at a distance  $d$  from the lens center:

$$\mathcal{G}_{alpha} : (x, y, d) \mapsto \alpha$$

with  $\alpha$  an alpha blending value in  $[0, \alpha_{FT}]$ ,  $\alpha_{FT}$  being the lowest translucence level used in the lens' flat-top. Note that it does not necessarily have to be 1.0 (opaque), though it will often be close to it. Drop-off function  $\mathcal{G}_{alpha}$  is usually a monotonically decreasing function. Again, this is not a requirement, but other types of functions may introduce discontinuities in the blending gradient.

The rendering of a point  $(x, y)$  in the final viewing window is then defined through the blending function  $b$ :

$$b(x, y) = \begin{cases} (x_c + \frac{x-x_c}{MM}, y_c + \frac{y-y_c}{MM}) \otimes_{\alpha_{FT}} (x, y) & \{\forall(x, y)|d(x, y) \leq R_I\} \quad (1) \\ (x_c + \frac{x-x_c}{MM}, y_c + \frac{y-y_c}{MM}) \otimes_{\mathcal{S}_{alpha}(x, y, d)} (x, y) & \{\forall(x, y)|R_I < d(x, y) < R_O\} \quad (2) \\ (x, y) & \{\forall(x, y)|d(x, y) \geq R_O\} \quad (3) \end{cases}$$

Figure 3 shows how translucence is used to transition between focus and context in what we call a **BLENDING** lens. This dimension offers an alternate way to smoothly transition between focus and context without resorting to spatial distortion, thus eliminating the drawbacks specifically associated with the latter. As we will discuss in the evaluation section, this transition type introduces problems of its own.

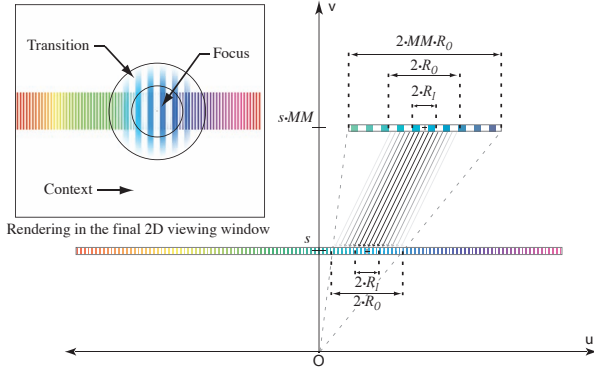


**Figure 3. Blending lens in a 1+1D space-scale diagram, and corresponding 2D rendering.**

### Time-based Transitions

The transition functions described in the previous sections make it possible to create a broad range of lenses. However, as is the case with most lenses reported in the literature, the properties of these lenses are defined statically. One notable exception is the Speed-coupled flattening lens [11] which uses the lens' dynamics (velocity and acceleration) to automatically control magnification: basically,  $MM$  decreases toward 1.0 as the speed of the lens (operated by the user) increases, therefore "flattening" the lens into the context, and increases back to its original value as the lens comes to a full stop. Speed-coupled flattening lenses have been demonstrated to outperform their static counterpart, and represent a first step in the direction of using time-dependent transitions to improve the usability of lenses.

The magnification factor of a lens ( $MM$ ) is an obvious parameter to control over time. There is no reason however to limit the use of the lens' dynamics to this one alone. Other candidates include the lens' radii  $R_I$  and  $R_O$ , as well as the lens' translucence value in its flat-top  $\alpha_{FT}$ .

We note  $\mathcal{F}(t)$  any time-based function returning a numerical value that can be used to dynamically change one or more of the above-mentioned lens properties. In the following we focus on one particular function: the lens' velocity and acceleration over time. This is however just one possible function

	MAGNIF. GLASS	FISHEYE	SPEED-C. FLAT.	BLENDING	SPEED-C. BLEND.
Magnif. Factor	$MM$	$MM$	$MM \cdot \mathcal{F}(t)$	$MM$	$MM$
Spatial drop-off	step function	Gaussian	Gaussian	step function	step function
$\alpha_{FT}$	1.0	1.0	1.0	$\alpha$	$\alpha \cdot \mathcal{F}(t)$
Blending drop-off	step function	step function	step function	Gaussian	step function

**Table 1. Properties of existing and new lenses in the design space**

of time, and we plan to investigate other functions in future work.

### Overall Lens Design Space

Spatial transitions and transitions based on translucence can be combined in a single lens, each with their own drop-off and distance functions. Additionally, several lens properties can be made time-dependent. This makes for a rather complex expression for computing the rendering of a point  $(x, y)$  seen through the lens, which reflects the richness of our new design space. Table 1 gives a summary of the properties of both existing and new lenses within this design space.

The first three lenses already exist in the literature. The **MAGNIFYING GLASS**, illustrated in Figure 1-a, consists only of a flat-top ( $R_O = R_I$ ) which occludes the immediate surroundings of the magnified region. **FISHEYE** denotes the common graphical fisheye lens. Here we use a Gaussian drop-off function to transition, through space only, between focus and context (Figures 1-b and 2). The **SPEED-COUPLED FLATTENING** lens is a variation on the one introduced by Gutwin [11], applied here to constrained lenses. It uses a simple interpolated low-pass filter inspired by the one of trailing widgets [8] as a time-based function to control the magnification factor based on the lens' velocity and acceleration.

The last two techniques are new contributions identified while exploring our design space. The **BLENDING** lens, illustrated in Figures 1-c and 3, can be seen as the simplest example of a translucence-based transition: it is like a **MAGNIFYING GLASS** that gradually blends into the context. Smoothness of transition is achieved without resorting to spatial distortion: context pixels gradually fade out as we get closer to the lens' center, while focus pixels gradually fade in.

The last lens, called **SPEED-COUPLED BLENDING**, is even closer to a **MAGNIFYING GLASS**. It shares all of its properties except that its  $\alpha_{FT}$  depends on the lens' movements. When still, the lens looks like a **MAGNIFYING GLASS**. But the flat-top becomes increasingly and uniformly translucent as the lens moves faster, becoming fully transparent beyond a given speed threshold  $S$ . The same type of low-pass filter as that governing the behavior of the **SPEED-COUPLED FLATTENING** lens is used. Figure 1-d shows a screenshot of a **SPEED-COUPLED BLENDING** lens moving at slow speed. Figure 4 illustrates the behavior of this lens when moving it from left to right in the scene introduced in the previous section: ( $t_1$ ) the lens stands still on the left side of the color spectrum; ( $t_2$ ) the user starts moving the lens to position it at the other end of the scene: the context can be seen through the focus (which

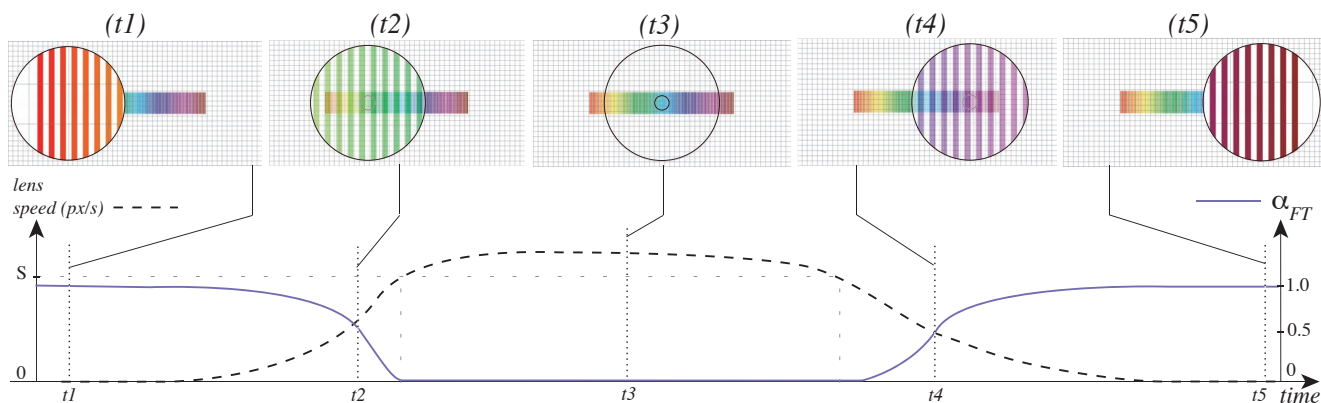


Figure 4. Speed-Coupled Blending Lens moving from left to right over time.

is itself still visible) by translucence; ( $t_3$ ) the lens is moved fast, beyond threshold speed  $S$ ; the focus is thus completely transparent: only the context is visible; ( $t_4$ ) the user slows down, the lens' focus gradually reappears; ( $t_5$ ) the user has reached the desired position, the lens comes to a full stop, and the focus is opaque again. A small inner circle can be noticed inside the lens at ( $t_2$ ), ( $t_3$ ) and ( $t_4$ ). This circle identifies, at the scale of the context, what region is magnified in the flat-top. The visibility of this translucent circle is controlled by  $1 - \alpha_{FT}$ : invisible when the lens stands still, it becomes more and more apparent as the lens moves faster, and conversely. This indicator was added as a result of a pilot study: we discovered that feedback, in the context view, of the position and size of the region to be magnified helped targeting objects more efficiently. The same type of indicator was then added to our version of the SPEED-COUPLED FLATTENING lens; in that case, the small circle expands and shrinks during lens movements, as its size directly depends on  $MM$ . This inherent instability makes it less convenient than its SPEED-COUPLED BLENDING counterpart, but it is still of great help when targeting an object.

BLENDING and SPEED-COUPLED BLENDING lenses are just two of several new interesting focus+context techniques that have been identified in the *Sigma lens* design space. The latter could actually be further extended to include other rendering techniques to achieve focus-context transitions, such as those based on multiblending [1], to highlight particular features of objects in the transition area. These are however still too computationally expensive to achieve acceptable frame rates on most personal computers, and are left as future work.

### EXPERIMENT 1: FOCUS TARGETING PERFORMANCE

We conducted an experiment to compare the performance and limits of the three existing and two new lenses described in the previous section. Participants were asked to perform a simple task, namely *focus targeting*, which consists in putting a given target in the flat-top of the lens. Focus targeting is one of the building blocks of many higher-level navigation tasks such as searching [24].

Focus targeting performance was evaluated at five different magnification factors ( $MM$ ). Higher magnification factors make the task increasingly difficult: (i) the transition area

becomes harder to understand as it must integrate a larger part of the world in the same rendering area, and (ii) it becomes harder to precisely position the target in the flat-top of the lens, the latter being controlled in the motor space of the context window. To test the limits of each lens, we included factors up to 14x.

### Apparatus

We used a Dell Precision 380 equipped with a 3 GHz Pentium D processor, an NVidia Quadro FX4500 graphics card, a 1600 x 1200 LCD monitor (21") and a Dell optical mouse. The program was written in Java 1.6 using the open source ZVTM toolkit [23] which offers a wide range of distortion lenses and could easily be extended to support translucence- and time-based transitions. The application was limited to a 1400 x 1200 window with a black padding of 100 pixels in order to accommodate instruction messages and simulate screen real-estate that would usually be taken by control and information widgets.

### Participants

Ten unpaid adult volunteers (7 male, 3 female), from 23 to 40 year-old (average 26.4, median 25), all with normal or corrected to normal vision, served in the experiment.

### Task and Procedure

Our focus targeting task consisted in acquiring a target in the flat-top of the lens as quick as possible. In our experimental setting, the lens was centered on the mouse cursor. The task ended when the participant clicked the left mouse button, provided that the target was fully contained within the flat-top. As focus targeting consists not only in correctly positioning the lens, but also in looking at the magnified target, additional conditions were imposed on some lenses to guarantee sufficient target visibility. The SPEED-COUPLED FLATTENING lens had to be magnifying enough ( $MM \geq 60\%$  of max. value), and the SPEED-COUPLED BLENDING lens had to be opaque enough ( $\alpha_{FT} \geq 0.4$ ). If all conditions were met when the participant clicked the mouse button for the first time, the targeting was counted as a *hit*, otherwise, as a *miss*. Each trial consisted in performing 24 successive focus targeting tasks. As illustrated in Figure 5, the targets were laid out in a circular manner. The order of appearance

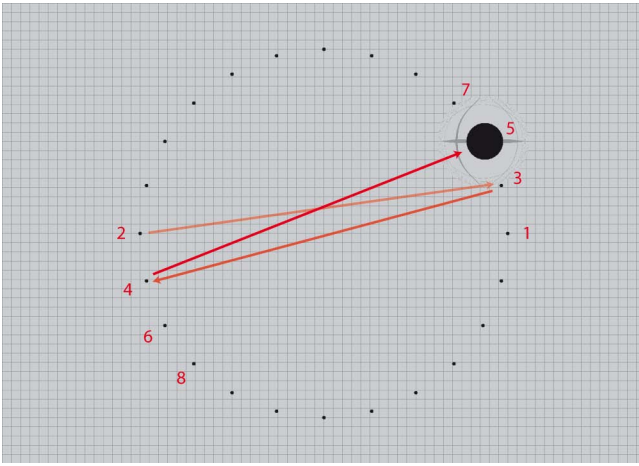


Figure 5. Exp. 1 & 2: Targets’ order of appearance in a trial (targets have been made twice their actual relative size for legibility purposes).

forced participants to perform focus targeting tasks in every direction, as recommended by the ISO9241-9 standard [18]. We decided to have only one target visible at a time, as we noticed during a pilot experiment in which all targets were visible that some participants were often taking advantage of the layout pattern to acquire the object set as the current target by positioning the lens relative to that object’s siblings.

Our experiment was a  $5 \times 5$  within-participant design: each participant had to perform several trials using each of the five lenses ( $Lens \in \{\text{MAGNIFYING GLASS, FISHEYE, BLENDING, SPEED-COUPLED FLATTENING, SPEED-COUPLED BLENDING}\}$ ) with five different magnification factors ( $MM \in \{2, 4, 6, 10, 14\}$ ). We grouped trials into five blocks, one per lens, so as not to disturb participants with too many changes between lenses. To avoid a non-controlled effect of order, we used a Latin square to compute five different orders of presentation for lenses and assigned two participants per order. Within a *Lens* block, each participant had to perform ten trials (i.e.  $10 \times 24$  focus targeting tasks), 2 trials with each of the five different values of  $MM$ . Trials within a block were presented in a random order after a training phase containing 3 trials ( $MM = 2, 6$  and  $14$ ), allowing participants to get familiar with a given lens before empirical measures were collected. The 24 targeting tasks of a trial had to be performed in a row, but participants were allowed to rest between trials. The first targeting task of each trial was ignored. A total of 11500 actual focus targeting tasks were thus taken into account in the analysis. The experimenter first introduced the task, and then each lens immediately before the corresponding block, and made sure that participants did understand how each one worked and how best to operate it.

### Predictions

We drew the following predictions based on each lens’ properties, the results of previous studies and a theoretical analysis of the motor movements involved in focus targeting.

**$H_1$  BLENDING lenses outperform FISHEYE lenses.** Transitioning through space introduces distortion that makes objects move away from the approaching lens focus before

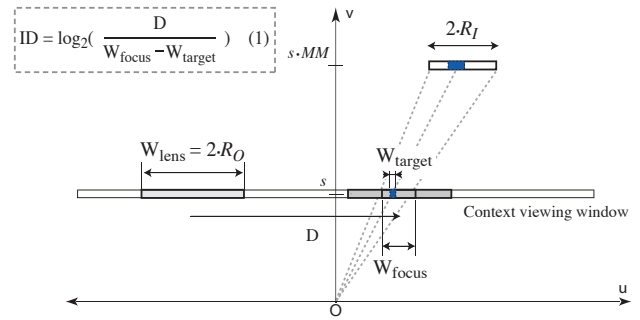


Figure 6. Focus Targeting Task in a space scale diagram.

moving toward it very fast, making focus targeting difficult [11]. Translucence-based transitions used in BLENDING lenses have their own problems, with a negative impact on targeting performance, but these might not be as strong as that commonly associated with distortion.

**$H_2$  SPEED-COUPLED FLATTENING and SPEED-COUPLED BLENDING lenses outperform all other lenses.** Each focus targeting task can be divided into two phases: in the first phase, the user moves the lens quickly to reach the target’s vicinity, while in the second phase, she moves it slowly to precisely position the target in the focus. In the first phase, the user is not interested in information provided in the focus region since she is trying to reach a distant object in the context as quick as possible. This hypothesis motivated the design of SPEED-COUPLED FLATTENING lenses and is supported by the results of the study conducted in [11]: SPEED-COUPLED FLATTENING lenses outperform FISHEYE lenses when performing focus targeting tasks ( $\text{SPEED-COUPLED FLATTENING} \geq \text{FISHEYE}$ )<sup>1</sup>. Here, we hypothesize that no matter the transition dimensions involved, providing a detailed view during the first phase is of limited value and has a negative effect on performance, leading to the conclusion that smoothly and automatically neutralizing the focus and transition regions during this phase, and then restoring them, can help the user. This leads to the following partial order:  $\text{SPEED-COUPLED FLATTENING} \geq \text{FISHEYE}$  and  $\text{SPEED-COUPLED BLENDING} \geq \text{MAGNIFYING GLASS}$ .

**$H_3$  Focus targeting is easier with MAGNIFYING GLASS lenses and SPEED-COUPLED BLENDING lenses.** From a pure motor perspective, the difficulty of a focus targeting task can be evaluated as a view pointing task in a fixed-scale interface [10]. We can thus use Formula (1) in Figure 6 to quantify the difficulty of moving the lens’ flat-top, of size  $W_{focus}$ , to a position where it will contain the target, of size  $W_{target}$ , initially located at a distance  $D$  from the lens’ center. Formula (1) computes the Index of Difficulty,  $ID$ , of our focus targeting task. The lens’ position in the context window is controlled in the visual and motor space of that window.  $W_{target}$ ,  $W_{focus}$  and  $D$  are thus expressed in context pixels: in our experiment,  $W_{target} = 8$  pixels and  $D = 800$  pixels, while  $W_{focus}$  depends on a given  $Lens \times MM$  condition:  $W_{focus} = (2 \times R_I) / MM$ . As  $MM$  increases, the size of  $W_{focus}$  decreases, making the task more difficult. For

<sup>1</sup> $L_1 > L_2$  means that  $L_1$  outperforms  $L_2$

lenses of equal size ( $R_O$ ), the size of the flat-top ( $R_I$ ), and thus  $W_{focus}$ , vary depending on the lens type. MAGNIFYING GLASS and SPEED-COUPLED BLENDING lenses are made of a flat-top only:  $W_{focus} = W_{lens} = 200$ , while other lenses have to accommodate the transition within the same overall area:  $W_{focus} = W_{lens}/2 = 100$  in our implementation. MAGNIFYING GLASS and SPEED-COUPLED BLENDING thus feature a larger flat-top than other lenses with the same overall size, consequently making focus targeting easier from a motor perspective:  $ID$  ranges from 3.2 to 6.3 for MAGNIFYING GLASS and SPEED-COUPLED BLENDING while it ranges from 4.2 to 8 for FISHEYE, SPEED-COUPLED FLATTENING and BLENDING. This reasoning however does not take into account non-motor aspects of the task which also depend on the type of lens used. For instance, occlusion caused by the always-opaque MAGNIFYING GLASS should increasingly hinder performance in the second phase of the task (precise positioning) as  $MM$  gets bigger:  $W_{focus}$  becomes smaller while  $W_{lens}$  remains constant, making the occlusion zone between focus and context on the path to the target larger, along with the chances of losing track of the target.

Altogether, these three hypotheses only provide a partial order of performance between the five lenses. One strong expectation is that the SPEED-COUPLED BLENDING lens will perform efficiently as it addresses many issues: it does not distort the representation, the dynamically controlled translucent flat-top reduces occlusion problems, and its large size makes the task easier from a motor perspective.

## Results and Discussion

Analysis of variance revealed a significant simple effect on number of errors (*miss*) for  $MM$  ( $F_{4,36} = 46, p < 0.0001$ ), for  $Lens$  ( $F_{4,36} = 6, p < 0.0001$ ), and a significant interaction effect on number of errors for  $Lens \times MM$  ( $F_{16,144} = 4, p < 0.0001$ ). As the mean number of errors for each lens and the total number of errors are low (from 0.05 for BLENDING to 0.02 for MAGNIFYING GLASS for a total of 380 *misses*, about 3%), we focus the following analyses on *hits* only. We verified that there was no effect of lens presentation order on time and observed that learning effects were not significant for each lens. We observed a significant simple effect on time for  $Lens$  ( $F_{4,36} = 66, p < 0.0001$ ). Tukey post hoc tests revealed that SPEED-COUPLED BLENDING is the fastest lens and SPEED-COUPLED BLENDING the slowest, while BLENDING, FISHEYE and SPEED-COUPLED FLATTENING do not significantly differ in terms of performance. We also observed a significant simple effect on time for  $MM$  ( $F_{4,36} = 648, p < 0.0001$ ) and a significant interaction effect on time for  $Lens \times MM$  ( $F_{16,144} = 88, p < 0.0001$ ). Figure 7 illustrates these results.

As expected, SPEED-COUPLED BLENDING performs better than all other lenses. Other predictions are only partially supported by the measures we collected. First,  $H_1$  is not supported. Our results reveal that FISHEYE  $\simeq$  BLENDING. Eliminating distortion by switching from a spatial transition to a smooth translucence-based transition does not seem to provide an advantage. Feedback collected from participants leads us to believe that this might be due to the high cognitive

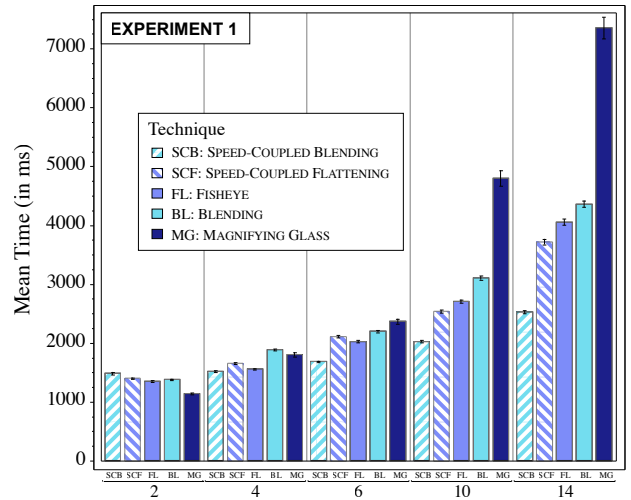


Figure 7. Mean completion time per  $Technique \times MM$  condition.

effort required to comprehend transitions based on gradually increasing translucence which, as opposed to distortion-based transitions, do not rely on a familiar physical metaphor.  $H_2$  is partially supported: (i) smoothly neutralizing and restoring the focus of a MAGNIFYING GLASS by making it translucent ( $\alpha_{FT}$  as a function of lens speed) does improve performance (SPEED-COUPLED BLENDING  $>$  MAGNIFYING GLASS); but (ii) flattening a fisheye ( $MM$  as a function of lens speed) does not yield a significant improvement over FISHEYE (SPEED-COUPLED FLATTENING  $\simeq$  FISHEYE). This last result is surprising since the study reported in [11] showed that SPEED-COUPLED FLATTENING outperforms FISHEYE for a *distortion level* of 5 (i.e.,  $MM = 6$ ). This inconsistency can be explained by taking a closer look at implementation details. First, we implemented SPEED-COUPLED FLATTENING as a constrained lens while it was implemented as a full-screen lens by Gutwin. In full-screen lenses, distortion affects the whole representation, which thus benefits more from the neutralization effect than constrained lenses that only affect a limited area. Second, as we require that  $MM \geq 60\%$  of max. value to end a trial, our task is a little bit longer than the one described in [11] in the SPEED-COUPLED FLATTENING condition, whereas this constraint does not exist in the FISHEYE condition. Finally,  $H_3$  is supported: SPEED-COUPLED BLENDING, with its large flat-top, outperforms all other lenses starting at  $MM = 4$ . Conversely the performance of MAGNIFYING GLASS goes down rapidly as  $MM$  gets higher. It becomes the worst lens starting at  $MM = 6$ , due to the earlier-mentioned negative effects of occlusion that make precise positioning difficult. It is interesting to note that for the lowest value of  $MM$ , MAGNIFYING GLASS outperforms all other lenses. Occlusion caused by the lens' opacity still causes the user to temporarily lose track of the target. But the occlusion zone is small at such low magnification. The negative impact of occlusion on performance is thus not significant compared to the positive impact of the larger flat top. Compared to SPEED-COUPLED BLENDING, MAGNIFYING GLASS also has the advantage of not requiring the user to wait several hundred milliseconds for the flat top to become opaque enough. In the particular case of very low magnification factors ( $MM \leq 2$ ), MAGNIFYING GLASS should thus be considered by interface designers.

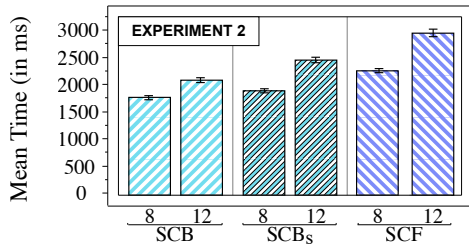


Figure 8. Mean completion time per  $MM \times Technique$  condition.

## EXPERIMENT 2: LENS SIZE AND MOTOR DIFFICULTY

Experiment 1 compared lenses with the same size ( $R_O$ ). We found that SPEED-COUPLED BLENDING lenses outperform SPEED-COUPLED FLATTENING lenses, and attributed this performance gain (i) to the large flat-top of the SPEED-COUPLED BLENDING lens which makes focus targeting easier from a motor perspective, and (ii) to the absence of distortion and reduction of occlusion effects through the coupling of focus translucence with lens speed. Experiment 2 aimed at better understanding the results of the previous experiment by identifying the contribution of both properties to this performance gain. We studied how SPEED-COUPLED BLENDING performed at two “extreme” sizes: 1) the lens has the same size as other lenses (as SPEED-COUPLED BLENDING in the first experiment), and 2) the lens has the same size as the flat-top of lenses which accommodate a transition area and thus feature a smaller flat-top, making focus targeting harder from a motor perspective as explained earlier. We called the latter SPEED-COUPLED BLENDING<sub>small</sub> and compared it to SPEED-COUPLED BLENDING and SPEED-COUPLED FLATTENING, both from the previous experiment. Apparatus was the same as before.

Lens	Lens size	Flat-top
SPEED-COUPLED FLATTENING (SCF)	200	100
SPEED-COUPLED BLENDING (SCB)	200	200
SPEED-COUPLED BLENDING <sub>small</sub> (SCBs)	100	100

## Participants

Six unpaid adult volunteers (5 male, 1 female), from 23 to 40 year-old (average 27.8, median 25.5), all with normal or corrected to normal vision, served in the experiment.

## Task and Procedure

The focus targeting task was exactly the same as the one used in Experiment 1. To reduce the length of this experiment, we picked two representative magnification factors:  $MM \in \{8, 12\}$ . This experiment was thus a  $3 \times 2$  within-participant design. We again grouped trials by lens type. We used a Latin square to compute three different presentation orders for lenses and assigned two participants per order. Each participant performed three *Lens* blocks. Within a block, each participant had to perform two trials (i.e.,  $2 \times 24$  focus targeting tasks), one trial per value of  $MM$ . For a given lens presentation order, one participant saw trials in order  $MM = 8$  then  $MM = 12$ , while the other one saw trials in order  $MM = 12$  then  $MM = 8$ . Each block began with a two-trial training phase, one per value of  $MM$ .

## Results and Discussion

Analysis of variance revealed a simple effect of *Technique* on time ( $F_{2,10} = 53, p < 0.0001$ ), a simple effect of  $MM$

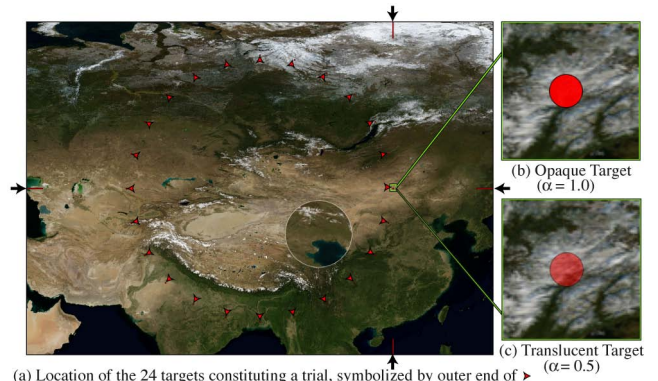


Figure 9. Exp. 3: targets are laid out radially (a), and can be either easily distinguished from the background (b), or blend into it (c).

on time ( $F_{1,5} = 230, p < 0.0001$ ), and an interaction effect of *Technique*  $\times$   $MM$  on time ( $F_{2,10} = 8, p < 0.0001$ ). Tukey post hoc tests revealed the following lens performance order: SPEED-C. BLENDING  $>$  SPEED-C. BLENDING<sub>small</sub>  $>$  SPEED-C. FLATTENING, as illustrated in Figure 8. These results show that even at the same level of motor difficulty (i.e., with equal flat-top sizes), the SPEED-COUPLED BLENDING lens still performs better than the SPEED-COUPLED FLATTENING lens. This means that interface designers are given several options to improve upon a classical lens such as FISHEYE: 1) they can either get a smaller but more efficient lens (in terms of focus targeting performance), saving screen real-estate for the context, 2) if the latter is not critical they can make the SPEED-COUPLED BLENDING lens occupy the same space as a FISHEYE would, further improving focus targeting performance, or 3) find a balance between these two solutions.

## EXPERIMENT 3: INFLUENCE OF TARGET VISIBILITY

Translucence can affect targeting performance [12], especially when targets are superimposed on a complex background such as a map or photograph. As the simple abstract world we used in the first two experiments might have hidden negative effects of translucence on lenses, we conducted a third experiment to check whether our comparative lens performance ordering was still valid when targeting objects that blend into a realistic background. Apparatus was the same as before.

## Participants

Eight unpaid adult volunteers (6 male, 2 female), from 23-28 years (avg. 24.7, med. 24.5), all with normal or corrected to normal vision, no color blindness, served in the experiment.

## Task and Procedure

The task was essentially the same as before, except for the fact that the 24 targets were laid out on a satellite photograph (Figure 9), and could either be filled with a fully opaque red color ( $\alpha = 1.0$ ) or with a translucent red ( $\alpha = 0.5$ ), in which case they blended into the background and were less easily identifiable. The satellite photograph was a 7000x5000 pixels portion of NASA’s Blue Marble Next Generation world map [31], providing appropriate levels of detail in both the focus and context regions. To limit the length of this ex-

periment, we discarded the poorly performing MAGNIFYING GLASS and picked only two representative magnification factors ( $MM \in \{8, 12\}$ ). This experiment was thus a  $4 \text{ Lens} \times 2 \text{ MM} \times 2 \text{ Opacity}$  within-participant design. Trials were again grouped by lens type. Participants performed four blocks which were presented in four varying orders computed through a Latin square. Each block was made of four trials (i.e.,  $4 \times 24$  focus targeting tasks), one per randomly distributed  $\text{Opacity} \times \text{MM}$  condition, and was preceded with a training phase of two trials ( $MM = 8, \text{Opacity} = 1$  and  $MM = 12, \text{Opacity} = 0.5$ ). As we were mainly interested in the effect of target visibility on the ending phase of our focus targeting task, we added two visual hints to help participants find the next target's location in the context, so as to control and reduce the associated visual search time as much as possible: 1) after a successful targeting, the next target appeared and its border flashed white for one second; 2) four red bars were located on the four edges of the context window (indicated by black arrows in Figure 9-a) so that the target was at their virtual intersection.

## Results and Discussion

Results were consistent with that of previous experiments, and matched participants' subjective preferences. Analysis of variance revealed a simple effect of *Technique* on time ( $F_{3,21} = 56, p < 0.0001$ ), a simple effect of *MM* on time ( $F_{1,7} = 212, p < 0.0001$ ), and an interaction effect of  $\text{Technique} \times \text{MM}$  on time ( $F_{3,21} = 12, p < 0.0001$ ). Our initial performance ordering was preserved. The only difference was that SPEED-COUPLED FLATTENING significantly outperformed FISHEYE (Figure 10). We tentatively attribute this higher significance to the more disturbing effects of distortion during lens movements on a complex background, to be confirmed by further evaluations.

Regarding the specific effect of target visibility, we found a simple effect of *Opacity* on time ( $F_{1,7} = 14, p = 0.007$ ), and an interaction effect of  $\text{Technique} \times \text{Opacity}$  on time ( $F_{3,21} = 6, p = 0.005$ ), confirming that lens performance does depend on this factor. However, Tukey HSD post hoc tests revealed that conditions  $\text{Opacity} = 0.5$  and  $\text{Opacity} = 1$  were in two different groups only for the BLENDING lens. This result is not unexpected as the BLENDING lens can be prone to visual interference between focus and context in the transition region depending on the nature of the representation, especially when non-contrasted objects are targeted. No matter how aesthetically pleasing (several participants noted that it produced very nice graphical renderings), the BLENDING lens suffers from its earlier-mentioned lack of reliance on a familiar physical metaphor, and proneness to visual interference in the transition region. The SPEED-COUPLED BLENDING lens, however, does not suffer from these problems, as its use of translucence is very different: it can be seen as a magnifying glass whose content smoothly fades out to prevent occlusion at focus targeting time.

## CONCLUSION

*Sigma lenses* form a rich and unified design space which includes a wide range of constrained lenses, from those that transition between focus and context through the spatial di-

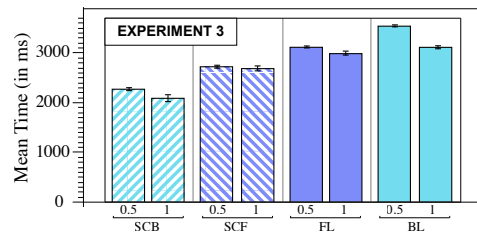


Figure 10. Mean completion time per  $\text{Opacity} \times \text{Technique}$  condition.

mension only, to new ones that achieve this transition using a combination of up to three dimensions among space, time, and translucence. We compared two such new lenses with three representatives of the first category using a focus targeting task. Empirical data revealed that our new SPEED-COUPLED BLENDING lens outperforms all other lenses.

These results encourage us to further investigate the use of non-spatial dimensions to transition between focus and context. First and foremost, the exploration of our design space has revealed several potentially interesting new lenses, based on innovative combinations of space and translucence, on the coupling of lens speed with properties such as its radii, or on the use of time-based functions other than lens speed. Secondly, we have seen that, depending on the lens and task studied, non-motor aspects can have a significant influence on performance, e.g., flat-top size and legibility, occlusion and search (depending on layout). We thus plan to formally evaluate lenses based on a wider range of tasks, including high-level cognitive ones.

## Acknowledgements

We wish to thank Olivier Bau, Michel Beaudouin-Lafon, Olivier Chapuis, Andy Cockburn, as well as Sheelagh Carpendale, Yves Guiard, Gonzalo Ramos, Dan Vogel, and the anonymous reviewers for their feedback.

## REFERENCES

1. P. Baudisch and C. Gutwin. Multiblending: displaying overlapping windows simultaneously without the drawbacks of alpha blending. In *CHI '04: Proc. Human Factors in Computing Systems*, pages 367–374. ACM Press, 2004.
2. E. Bier, M. Stone, K. Pier, W. Buxton, and T. DeRose. Toolglass and magic lenses: the see-through interface. In *SIGGRAPH '93: Proc. Computer graphics and interactive techniques*, pages 73–80. ACM Press, 1993.
3. M. S. T. Carpendale, D. J. Cowperthwaite, and F. D. Fracchia. 3-dimensional pliable surfaces: for the effective presentation of visual information. In *UIST '95: Proc. ACM Symp. on User Interface Software and Technology*, pages 217–226. ACM Press, 1995.
4. M. S. T. Carpendale, D. J. Cowperthwaite, and F. D. Fracchia. Making distortions comprehensible. In *VL '97: Proc. of the 1997 IEEE Symp. on Visual Languages*, page 36. IEEE Comput. Soc., 1997.
5. M. S. T. Carpendale and C. Montagnese. A framework for unifying presentation space. In *UIST '01: Proc.*

- ACM Symp. on User Interface Software and Technology*, pages 61–70. ACM Press, 2001.
6. S. Carpendale, J. Ligh, and E. Pattison. Achieving higher magnification in context. In *UIST '04: Proc. ACM Symp. on User Interface Software and Technology*, pages 71–80. ACM Press, 2004.
  7. D. A. Cox, J. S. Chugh, C. Gutwin, and S. Greenberg. The usability of transparent overview layers. In *CHI 98 conference summary on Human factors in computing systems*, pages 301–302. ACM Press, 1998.
  8. C. Forlines, D. Vogel, and R. Balakrishnan. Hybridpointing: fluid switching between absolute and relative pointing with a direct input device. In *UIST '06: Proc. ACM Symp. on User Interface Software and Technology*, pages 211–220. ACM Press, 2006.
  9. G. W. Furnas and B. B. Bederson. Space-scale diagrams: understanding multiscale interfaces. In *CHI '95: Proc. Human Factors in Computing Systems*, pages 234–241. ACM Press/Addison-Wesley, 1995.
  10. Y. Guiard and M. Beaudouin-Lafon. Target acquisition in multiscale electronic worlds. *Int. J. Hum.-Comput. Stud.*, 61(6):875–905, Dec. 2004.
  11. C. Gutwin. Improving focus targeting in interactive fisheye views. In *CHI '02: Proc. Human Factors in Computing Systems*, pages 267–274. ACM Press, 2002.
  12. C. Gutwin, J. Dyck, and C. Fedak. The effects of dynamic transparency on targeting performance. In *Graphics Interface*, pages 105–112. A K Peters, 2003.
  13. C. Gutwin and C. Fedak. A comparison of fisheye lenses for interactive layout tasks. In *Graphics Interface*, pages 213–220. A K Peters, 2004.
  14. C. Gutwin and A. Skopik. Fisheyes are good for large steering tasks. In *CHI '03: Proc. Human Factors in Computing Systems*, pages 201–208. ACM Press, 2003.
  15. B. L. Harrison, H. Ishii, K. J. Vicente, and W. A. S. Buxton. Transparent layered user interfaces: an evaluation of a display design to enhance focused and divided attention. In *CHI '95: Proc. Human Factors in Computing Systems*, pages 317–324. ACM Press/Addison-Wesley Publishing Co., 1995.
  16. K. Hornbæk, B. B. Bederson, and C. Plaisant. Navigation patterns and usability of zoomable user interfaces with and without an overview. *ACM Trans. Comput.-Hum. Interact.*, 9(4):362–389, 2002.
  17. T. Igarashi and K. Hinckley. Speed-dependent automatic zooming for browsing large documents. In *UIST '00: Proc. ACM Symp. on User Interface Software and Technology*, pages 139–148. ACM Press, 2000.
  18. ISO. 9241-9 Ergonomic requirements for office work with visual display terminals (VDTs)-Part 9: Requirements for non-keyboard input devices. *International Organization for Standardization*, 2000.
  19. T. A. Keahey and E. L. Robertson. Techniques for non-linear magnification transformations. In *INFOVIS '96: IEEE Symp. on Information Visualization*, pages 38–45. IEEE Computer Society, 1996.
  20. H. Lieberman. Powers of ten thousand: navigating in large information spaces. In *UIST '94: Proc. ACM Symp. on User Interface Software and Technology*, pages 15–16. ACM Press, 1994.
  21. J. D. Mackinlay, G. G. Robertson, and S. K. Card. The perspective wall: detail and context smoothly integrated. In *CHI '91: Proc. Human Factors in Computing Systems*, pages 173–176. ACM Press, 1991.
  22. C. North and B. Shneiderman. Snap-together visualization: a user interface for coordinating visualizations via relational schemata. In *AVI '00: Proc. working Conf. on Advanced Visual Interfaces*, pages 128–135. ACM Press, 2000.
  23. E. Pietriga. A Toolkit for Addressing HCI Issues in Visual Language Environments. In *VL/HCC'05: IEEE Symp. on Visual Languages and Human-Centric Computing*, pages 145–152. IEEE Comput. Soc., 2005.
  24. E. Pietriga, C. Appert, and M. Beaudouin-Lafon. Pointing and Beyond: an Operationalization and Preliminary Evaluation of Multi-scale Searching. In *CHI '07: Proc. Human Factors in Computing Systems*, pages 1215–1224. ACM Press, 2007.
  25. C. Plaisant, D. Carr, and B. Shneiderman. Image-browser taxonomy and guidelines for designers. *IEEE Software*, 12(2):21–32, 1995.
  26. T. Porter and T. Duff. Compositing digital images. In *SIGGRAPH '84: Proc. Comput. graphics and interact. techniques*, pages 253–259. ACM Press, 1984.
  27. G. Ramos, A. Cockburn, R. Balakrishnan, and M. Beaudouin-Lafon. Pointing lenses: facilitating stylus input through visual-and motor-space magnification. In *CHI '07: Proc. Human Factors in Computing Systems*, pages 757–766. ACM Press, 2007.
  28. G. G. Robertson and J. D. Mackinlay. The document lens. In *UIST '93: Proc. ACM Symp. on User Interface Softw. and Tech.*, pages 101–108. ACM Press, 1993.
  29. M. Sarkar and M. H. Brown. Graphical fisheye views. *Communications of the ACM*, 37(12):73–83, 1994.
  30. M. Sarkar, S. S. Snibbe, O. J. Tversky, and S. P. Reiss. Stretching the rubber sheet: a metaphor for viewing large layouts on small screens. In *UIST '93: Proc. ACM Symp. on User Interface Software and Technology*, pages 81–91. ACM Press, 1993.
  31. R. Stockli, E. Vermote, N. Saleous, R. Simmon, and D. Herring. The Blue Marble Next Generation - A true color earth dataset including seasonal dynamics from MODIS. Published by the NASA Earth Observ., 2005.
  32. C. Ware and M. Lewis. The DragMag image magnifier. In *CHI '95 conference companion, Human Factors in Computing Systems*, pages 407–408. ACM Press, 1995.